

# Detecting Lead Ion in Water with Boron-Doped Diamond Film Electrode

Xuanhao ZHANG <sup>a</sup>, Zhijun LI <sup>a,b</sup>, Shengxiang ZHANG <sup>b</sup>, Jinyuan LI <sup>b</sup>, Chenxiu FU <sup>c</sup>,  
Liang WU <sup>b</sup>, Xinghong Liu <sup>b</sup> and Xiang YU <sup>a,1</sup>

<sup>a</sup> Hainan QiandaZhicheng Culture Media Co., Ltd, No.2 Shimao East Road, Haikou  
570125, Hainan Province, China

<sup>b</sup> School of Materials Science and Technology, China University of Geosciences  
(Beijing), 29 Xueyuan Road, Haidian, Beijing 100083, China

<sup>c</sup> Beijing ConST Instruments Technology Inc., Yard 3 Fengxiu Middle Road, Haidian,  
Beijing 100094, China

**Abstract.** Monitoring  $Pb^{2+}$  content in drinking water is an important measure to safeguard water safety for residents. To overcome drawbacks available electrochemical sensors, this work attempts to fabricate a boron-doped diamond (BDD) electrode for detecting  $Pb^{2+}$  in water. A systematic investigation was conducted on microstructural and electrochemical performances of BDD electrode. The results show that, diamond grains arrange well on BDD electrode surface. The electrode exhibits a high electrochemical active surface area and low charge transfer resistance, favorable to accelerate the stripping reaction process of  $Pb^{2+}$ . BDD electrode has a low detection limit in optimized parameter set. Also, the BDD electrode has a good anti-interference ability. The designed BDD electrode is expected to be applicable for monitoring  $Pb^{2+}$  content in waters.

**Keywords.** Boron-doped diamond, electrode, water detection, heavy metal pollutant

## 1. Introduction

Rapid development of industrial society has caused serious water pollution, among which heavy metal pollutants have threatened the drinking water safety of hundreds of millions of people around the world [1].  $Pb^{2+}$  is a typical heavy metal pollutant because of its difficult degradation and high toxicity [2]. Detection of  $Pb^{2+}$  level in drinking water is thus important to ensure people's drinking water safety.

At present, liquid chromatography, atomic absorption spectrometry and other methods have been applied to detect trace  $Pb^{2+}$  in drinking water [3]. It is worth mentioning that electrochemical analysis technology shows good application potential for water quality monitoring because of its high sensitivity and fast signal response [4]. It is of great significance to develop water quality monitoring sensors based on electrochemical analysis technology. Boron doped diamond (BDD) has been given much attention as a new electrode material. It combines good physical and chemical properties of diamond and advanced functional properties of semiconductors, such as high hardness,

---

<sup>1</sup> Xiang Yu, Corresponding author, School of Materials Science and Technology, China University of Geosciences (Beijing), 29 Xueyuan Road, Haidian, Beijing 100083, China; E-mail: yuxiang@cugb.edu.cn.

good chemical stability and electrochemical properties. At present, it has been applied in the fields of supercapacitors, electrochemical sensors and so on [5]. The heavy metal analysis electrode developed based on BDD is expected to achieve high stability and reliability of water quality monitoring. However, there is still a lack of systematic research on using BDD electrode to detect  $\text{Pb}^{2+}$  content in drinking water.

In this work, a BDD electrode is prepared on the titanium substrate to detect trace  $\text{Pb}^{2+}$  in water. Microstructural and electrochemical behaviors of the BDD electrode are investigated along with its heavy metal analysis ability, so as to evaluate the application potential of BDD electrode in field of heavy metal monitoring for drinking water.

## 2. Experimental Section

### 2.1. Reagents and Instruments

Reagents used were of analytical grade. Ion standard solution was purchased from National Institute of Standards and Materials, and concentration as required for the solution to be tested was set by mixing with ultrapure water. BDD film electrode was prepared in a system of hot-filament chemical vapor deposition (HFCVD). Micromorphology of the electrode was observed using scanning electron microscope (SEM). The binding structure was detected by Raman confocal microscope. Electrochemical test was carried in electrochemical workstation.

### 2.2. Preparation of BDD Electrode

Titanium metal slice was used as substrate of BDD electrode. The cleaned substrate was placed in a diamond seed solution (5 gND/20 ml ethanol) for 10 min for seeding treatment. The substrate was then dried and placed in HFCVD chamber for deposition. Diboron trioxide was dissolved in ethanol as doping boron source, and was brought into the chamber through hydrogen gas. In nucleation stage, methane was used as carbon source, hydrogen was used as etching gas, and the ratio of  $\text{H}_2:\text{CH}_4$  was set as 10:1000 sccm for 0.5 h. In growth stage, gas flow of  $\text{H}_2$  (bubbling) was adjusted as  $\text{C}_2\text{H}_5\text{OH}+\text{H}_2+\text{B}_2\text{O}_3:\text{H}_2=25:50:1000$  sccm for 7.5 h. Main deposition parameters included C/H ratio (2.4%) , B/C ratio (6000ppm), deposition pressure (3 KPa) and deposition temperature (700 °C).

### 2.3. Electrochemical Measurement

BDD film was used as working electrode ( $10*10 \text{ mm}^2$ ), saturated glycerol electrode was used as reference electrode (3M KCl), and platinum sheet was used as counter electrode ( $10*15 \text{ mm}^2$ ). Cyclic Voltammetry (CV) test was used to investigate the electrode potential window, background current, and reaction kinetics in electrolytes of 0.1 M  $\text{Na}_2\text{SO}_4$  solution and 0.1 M  $\text{K}_3[\text{Fe}(\text{CN})_6]$  solution. Electrochemical impedance spectroscopy (EIS) was used to detect the electrochemical reaction process in frequency range of  $10^{-2}$ - $10^5$  Hz. Square wave dissolution voltammetry (SWASV) was used to assess  $\text{Pb}^{2+}$  in the water under condition of amplitude of 20 mV, step potential of 4 mV, and deposition potential of -0.8 V.

### 3. Results and Discussion

#### 3.1. Structural Characterization of BDD Electrode

Figure 1(a) shows the Raman spectra of the prepared BDD electrode on the surface and at the interface. In figure 1(a), the diamond phase achieves boron doping on the BDD surface. For the interface of the BDD electrode, two characteristic peaks can be observed at  $1334\text{ cm}^{-1}$  and  $1580\text{ cm}^{-1}$ , corresponding to the D (diamond) band ( $sp^3$ -C) and the G (graphite) band ( $sp^2$ -C), respectively [6]. The D band is a first order Raman characteristic peak of the diamond phase and can be used as direct evidence to determine the formation of diamond. The G band is caused by impurity phases such as amorphous carbon in the BDD. The G-band evident at the interface indicates poor phase formation during the initial growth phase of the BDD film.

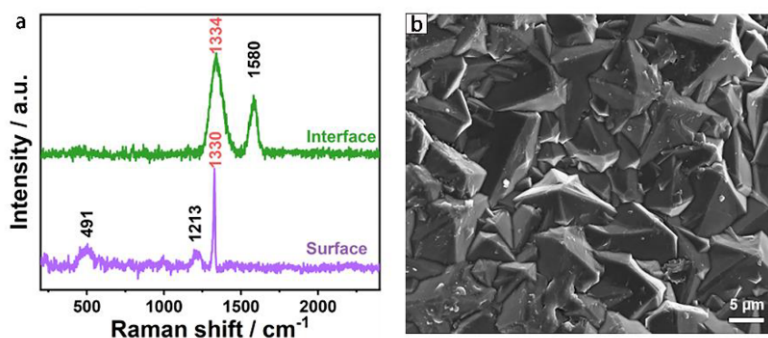


Figure 1. Structure of BDD electrode. (a) Raman spectra; (b) SEM image.

At the surface of the BDD electrode, there is no G-peak at  $1580\text{ cm}^{-1}$ , indicating an improved formation of the diamond phase. In addition, at  $491\text{ cm}^{-1}$ , a new characteristic peak appears, which can be attributed to phonon scattering due to the lattice change after doping with boron [7]. At the same time, the D-peak on the BDD surface at  $1330\text{ cm}^{-1}$ , shows a "blue shift" compared to the interface. This phenomenon is due to the "Fano" effect caused by boron doping. Together, these two phenomena confirm that boron was successfully doped into the diamond lattice to form the BDD film. BDD electrodes of this structure are expected to enhance detection performance.

Subsequently, the microscopic morphology of the BDD electrode was observed using SEM. Figure 1(b) shows the SEM image of the electrode. As shown in figure 1(b), the average size of the diamond grains is approximately  $8\text{ }\mu\text{m}$  and the grain morphology is a regular tetrahedral structure. The tetrahedral structure is a typical morphological feature of diamond grains with a (111) crystal plane, which indicates that the film has a preferential orientation along the (111) crystal plane. The (111) crystal plane is a surface where element B is easily exposed, improving the detection of heavy metals. In short, the favorable micro-morphology, and the preferential orientation of the film combine to promote good electrochemical analysis.

### 3.2. Electrochemical Characterization of BDD Electrode

Good electrochemical behavior is a guarantee for efficient detection of heavy metals at the BDD electrode. The potential window and background current of the BDD electrode were measured by cyclic voltammetry, as shown in figure 2. As can be seen from figure 2, the BDD electrode is free of hydrogen evolution and oxygen absorption reactions in the potential range of -1.2 V to +1.0 V. The electrode potential window is as high as 2.2 V. This wide potential window is due to the weak adsorption of  $sp^3$ -C on the BDD electrode to reaction intermediates in solution. A potential window of 2.2 V can adequately guarantee the dissolution analysis of lead at the BDD electrode<sup>2+</sup>. On the other hand, the low background current of the electrode represents a low electric double layer capacitance that may hinder charge transfer on the electrode surface.

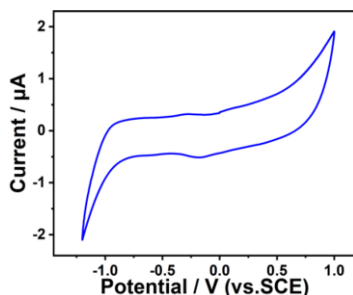


Figure 2. Cyclic voltammetry characteristic curve of BDD electrode in 0.1 M Na<sub>2</sub>SO<sub>4</sub> solution.

### 3.3. Determination of Trace Pb<sup>2+</sup> in Water

#### 3.3.1. Dissolution Parameter Optimization

In order to obtain a better signal response at the BDD electrode, two specifically chosen experimental parameters, namely the enrichment time and the scanning frequency, were optimized in turn at a Pb<sup>2+</sup> concentration of 30 ppb. Figure 3(a) shows the dissolution peak current values for the four enrichment times. In figure 3(a), the signal response tends to increase and then decay with increasing enrichment time. The electrodes show the lowest signal response at an enrichment time of 50 second. Extending the enrichment time enhances the signal response as the enrichment time extends, the current signal intensity gradually increases to its maximum. Afterwards, when the enrichment time extends to 200 s, the electrode signal response become poor. Impurity ions in the solution system gradually participate in the dissolution process, interfering with the reduction of the ions to be measured at the electrode and suppressing the current value. Therefore, 150 s is chosen as the preferred enrichment time because of its highest signal response.

Scan frequency is another important factor affecting the dissolution signal. It can affects the signal response of the ion to be measured by influencing the input process of the voltage signal. For this reason, the peak dissolution current values for Pb<sup>2+</sup> are examined at four scan frequencies (25Hz, 50Hz, 100Hz, and 125Hz) in turn. Figure 3(b) shows the peak dissolution current values at the four scanning frequencies. In figure 3(b), the signal enhances and then decays as the scan frequency increases, with the maximum value obtained at 50 Hz. This is the scan frequency that ensures adequate reduction and oxidation of the ions to be measured and makes the peak current reach its maximum

value. The signal response then decreases slightly as the scan frequency further increased to 100 and 125 Hz. In this way, an enrichment time of 150 seconds and a scanning frequency of 50 Hz are chosen as the optimized dissolution parameters for subsequent experiments.

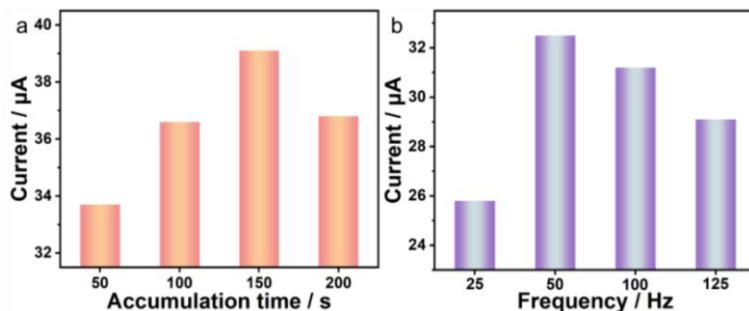


**Figure 3.** Effect of enrichment time and scan frequency on signal response of BDD electrode. (a) Dissolved peak current values of BDD electrode for  $\text{Pb}^{2+}$  at four enrichment times; (b) Dissolved peak current values of BDD electrode for  $\text{Pb}^{2+}$  at four scanning frequencies.

### 3.3.2. Sensitivity Detection

Detection capability of the electrodes is a unique property for assessing their suitability for practical water analysis. An optimized combination of dissolution parameters was used to detect concentrations of  $\text{Pb}^{2+}$  solutions with gradient variations. Figure 4(a) shows the linear fit curve between the  $\text{Pb}^{2+}$  content and its peak dissolution current value. As shown in figure 4(a), the content of  $\text{Pb}^{2+}$  remained linear to the dissolution peak current over the range of 5–30 ppb, with a linear correlation ( $R^2$ ) of up to 0.994 for the fitted curve. The standard curve equation was  $y = 1.45x - 3.64$ , as reflected by the slope of the standard curve. The detection limit of the electrode ( $3N/S$ ) was further calculated to be 2.62 ppb. The above performance indicates that the prepared BDD electrode can achieve sensitive detection of trace amounts of lead in water.

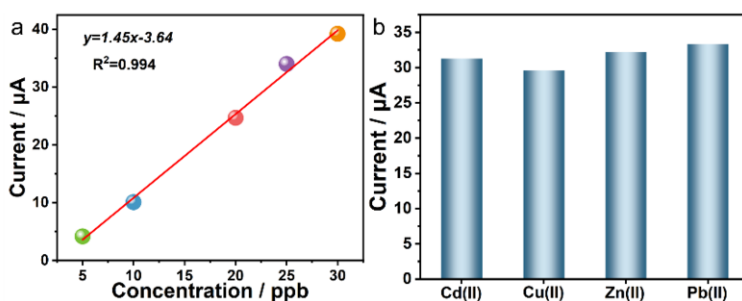


**Figure 4.** Detection performance of BDD for  $\text{Pb}^{2+}$ . (a) Linear fitting curve between  $\text{Pb}^{2+}$  content and dissolution peak current; (b) Dissolution peak current before and after addition of interfering ions.

### 3.3.3. Anti-interference Ability

The complex composition of actual water bodies is an obstacle to the practical application of BDD electrodes. Good immunity to interference can ensure that the electrodes perform highly selective analysis and cope with complex detection

environments.  $\text{Cd}^{2+}$ ,  $\text{Cu}^{2+}$  and  $\text{Zn}^{2+}$  were added to the system of solutions to be tested in turn for electrochemical analysis, and their immunity to interference was evaluated by recording the changes in the peak current values of dissolved  $\text{Pb}^{2+}$ . Figure 4(b) shows the peak current values of dissolved  $\text{Pb}^{2+}$  solution in pure form and the mixed solution with the addition of  $\text{Cd}^{2+}$ ,  $\text{Cu}^{2+}$  and  $\text{Zn}^{2+}$ . As shown in figure 4(b), the highest signal intensity is observed for the pure  $\text{Pb}^{2+}$  solution, and the dissolution signal of  $\text{Pb}^{2+}$  does not change significantly after the addition of  $\text{Cd}^{2+}$ ,  $\text{Cu}^{2+}$  and  $\text{Zn}^{2+}$ , and only a slight attenuation occurs. This result demonstrates the good immunity of the BDD electrode to interference and provides direct evidence for its wide application in real water bodies.

#### 4. Conclusion

In this work, BDD film electrode is developed to detect trace  $\text{Pb}^{2+}$  in water. Based on systematical investigation of the microstructural and electrochemical performances, dissolution parameters of BDD electrode are optimized, and heavy metal detection of the electrode is also evaluated. Main conclusions include: (1) The diamond grains arranged and submerged on BDD electrode surface, and featured high phase quality. (2) The electrode has a wide potential window and low background current. (3) The electrode shows excellent selectivity for  $\text{Pb}^{2+}$  of  $1.45 \mu\text{A L } \mu\text{g}^{-1} \text{cm}^{-2}$  in linear range of 5-30 ppb, and low detection limit of 2.62 ppb. BDD electrode developed in this work is expected to achieve stable and reliable monitoring of  $\text{Pb}^{2+}$  content in drinking water.

#### References

- [1] Gleick PH. Global freshwater resources: Soft-path solutions for the 21st Century. *Science* 2003 Nov; 302(5650): 1524-1528.
- [2] Chowdhury S, Mazumder MAJ, Al-Attas O, Husain T. Heavy metals in drinking water: Occurrences, implications, and future needs in developing countries. *Sci. Total Environ.* 2016 Nov; 569: 476-488.
- [3] Zhang YN, Sun Y, Cai L, Gao YP, Cai Y. Optical fiber sensors for measurement of heavy metal ion concentration: A review. *Measurement.* 2020 Jul; 158: 107742.
- [4] Lu YY, Liang XQ, Niyungeko C, Zhou JJ, Xu JM, Tian GM. A review of the identification and detection of heavy metal ions in the environment by voltammetry. *Talanta.* 2018 Feb; 178: 324-338.
- [5] Guo CY, Zheng JG, Deng HW, Shi PH, Zhao GH. Photoelectrocatalytic interface of boron-doped diamond: Modification, functionalization and environmental applications. *Carbon.* 2021 Apr; 175: 454-466.
- [6] Mortet V, Taylor A, Zivcova ZV, Machon D, Frank O, Hubik P, Tremouilles D, Kavan L. Analysis of heavily boron-doped diamond Raman spectrum. *Diam. Relat. Mater.* 2018 Sep; 88: 163-166.
- [7] Ashcheulov P, Šebera J, Kovalenko A, Petrák V, Fendrych F, Nesládek M, Taylor A, Živcová ZV, Frank O, Kavan L. Conductivity of boron-doped polycrystalline diamond films: Influence of specific boron defects. *Eur. Phys. J. B.* 2013 Oct; 86(10): 443-451.